Investment of needle nitrogen to photosynthesis controls the nonlinear productivity response of young Chinese fir trees to nitrogen deposition

Renshan Li [a, b], Dan Yu [b], Yankuan Zhang [a, f], Jianming Han [b], Weidong Zhang [a, c, *], Qingpeng Yang [a, c, *], Arthur Gessler [d], Mai-He Li [a, d], Ming Xu [e], Xin Guan [a, c], Longchi Chen [a, c], Qingkui Wang [a, c], Silong Wang [a, c]

[a] *Huitong Experimental Station of Forest Ecology, CAS Key Laboratory of Forest Ecology and Management, Institute of Applied Ecology, Shenyang 110016, China*

[b] *Life Science Department, Luoyang Normal University, Luoyang 471934, China*

[c] *Huitong National Research Station of Forest Ecosystem, Huitong 418307, China*

[d] *Forest Dynamics, Swiss Federal Research Institute WSL, Zuercherstrasse 111, 8903 Birmensdorf, Switzerland*

[e] *Henan Key Laboratory of Earth System Observation and Modeling, Henan University, Kaifeng 475004, China*

[f] *University of Chinese Academy of Sciences, Beijing 100049, China*

Author for correspondence: Weidong Zhang; Qingpeng Yang

E-mail address: wdzhang@iae.ac.cn; yqp226@iae.ac.cn.

This document is the accepted manuscript version of the following article:
Li, R., Yu, D., Zhang, Y., Han, J., Zhang, W., Yang, Q., … Wang, S. (2022). Investment of needle nitrogen to photosynthesis controls the nonlinear productivity response of young Chinese fir trees to nitrogen deposition. Science of the Total Environment, 840, 156537 (9 pp.). https://doi.org/10.1016/j.scitotenv.2022.156537

Abstract

Plant carbon (C) assimilation is expected to nonlinearly increase with continuously increasing nitrogen (N) deposition, causing a N saturation threshold for productivity. However, the response of plant productivity to N deposition rates and further the N saturation threshold still await comprehensive quantization for forest ecosystem. Here, we tested the effect of N addition on aboveground net primary productivity (ANPP) of three-year old Chinese fir (*Cunninghamia lanceolata*) trees by adding N at 0, 5.6, 11.2, 22.4, and 44.8 g N m^{-2} yr^{-1} for 2.5 years. The N saturation threshold was estimated based on a quadratic-plus-plateau model. Results showed that ANPP transitioned from an increasing stage with increasing N addition rate to a plateaued stage at an N rate of 16.3 g N m^{-2} yr^{-1}. The response of ANPP to N addition rates was well explained by the net photosynthetic rates of needles. Results from the dual isotope measurement [simultaneous determination of needle stable carbon ($\delta^{13}C$) and oxygen ($\delta^{18}O$) isotopes] indicated that the photosynthetic capacity, rather than the stomatal conductance, mediated the response of photosynthesis and ANPP of the young Chinese fir trees to N addition. Accordingly, the amount of needle N partitioning to water-soluble fraction, which is associated with the photosynthetic capacity, also responded to N enrichment with a nonlinear increase. Our study will contribute to a more accurate prediction on the influence of N deposition on C cycles in Chinese fir plantations.

Key words: Dual isotope approach; Foliar age effect; Forest C uptake; Nitrogen amendment

Graphic Abstract

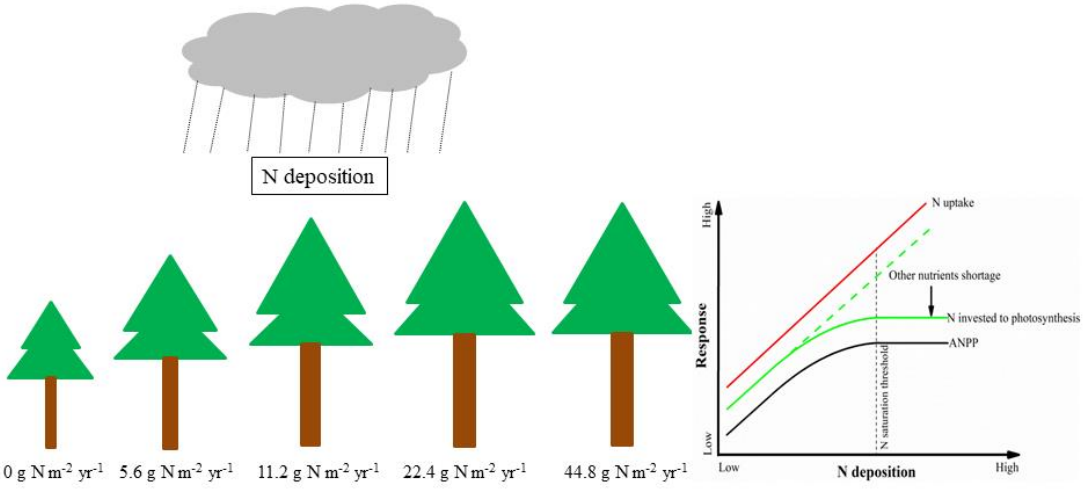

1 Introduction

The world is experiencing intense atmospheric nitrogen (N) deposition caused by extensive industrial emissions, fossil fuel combustion, and agricultural fertilization (Aber et al., 1989; Vitousek et al., 1997; Liu et al., 2013). Increased N deposition can provide an extra fertilizer source for plant growth, since N is a major component of enzyme ribulose-1·5-bisphosphatecarboxylase/oxygenase (Rubisco) and other photosynthetic enzymes which regulate the photosynthetic capacity (Högberg, 2007; Yu et al., 2019). It has long been proposed that there is a N saturation threshold for plant photosynthetic carbon (C) gain, because a low-dose and appropriate increase of N input may satisfy plant demand, while an over-saturated N addition likely cause nutrient disorder and thus net photosynthesis reduction (Lu et al., 2018; Mao et al., 2018). However, little attention has been paid to the N saturation threshold in forest ecosystems (Wei et al., 2012; de Vries et al., 2014; Tian et al., 2016), mainly because most previous forest studies on this topic considered only two or three N addition

gradients, which did not support the estimation of the N saturation threshold (Bauer et al., 2001 & 2004; King et al., 2008; Talhelm et al., 2011; Krause et al., 2012; Hu et al., 2021).

The N saturation threshold can also be determined by possible water depletion following N addition. For example, N enrichment might increase tree growth, stimulating water consumption via transpiration and intercepting more precipitation that should have been absorbed by the soil, which further reduces foliar water supply and thus the stomatal conductance (Li et al., 2020 a). Lower stomatal aperture decreases the diffusion of CO_2 into the leaf, thereby constraining the photosynthetic response to N addition (McDowell et al., 2003). In an arid grassland ecosystem in northern China, Bai et al. (2010) reported that the decline in soil moisture following N addition constrained the response of aboveground productivity to N addition. Soil water depletion after N addition occurs not only in the arid regions, but also in the humid subtropical regions (Lu et al., 2018). It is unclear, however, to what extent the N induced soil water depletion in subtropical regions affects foliar stomatal openness and further the N saturation threshold, because water under normal conditions is not a limiting factor for plants grown in subtropical regions (Li et al., 2017).

The control of photosynthetic capacity and stomatal aperture on the N saturation threshold is confounded. Previous studies often separate the two mechanisms by simultaneously analyzing foliar photosynthetic rate and stomatal conductance and/or transpiration (Lu et al., 2018; Mao et al., 2018). However, those instantaneous gas exchange measurements are susceptible and sometimes insufficient to show the real

coupling between photosynthetic capacity and stomatal conductance (Li et al., 2020 b). These limitations can be overcome by a dual isotope approach, which provides time-integrated information about the coupling between C uptake and resource availability (Giuggiola et al., 2016). In C_3 plants, because of the discrimination of $^{13}CO_2$ by enzyme Rubisco, stable C isotope composition ($\delta\ ^{13}C$) of plant organic matter inversely correlate with the ratio of internal (ci) to atmospheric (ca) CO_2 concentrations (ci/ca) (Farquhar et al., 1982). Thus, $\delta\ ^{13}C$ can be regulated by both stomatal conductance and photosynthetic capacity, since ci is governed by the balance between CO_2 influx (supply) and carboxylation (consumption) within the leaf (Farquhar et al., 1989). The effects of stomatal conductance and carboxylation on foliar $\delta\ ^{13}C$ can be separated by the assessment of stable oxygen isotope composition ($\delta\ ^{18}O$) of plant organic matter, because $\delta\ ^{18}O$ is often negatively related to foliar stomatal conductance but is irrelevant to carboxylation (Scheidegger et al., 2000; Farquhar et al., 2007). To our best knowledge, however, only a few experiments have used this dual isotope approach to evaluate plant ecophysiological responses to N deposition (Talhelm et al., 2011; Krause et al., 2012).

Moreover, whether there are leaf age specific contributions to the N saturation threshold for productivity still awaits clarification. This knowledge gap would particularly limit to accurately predict the C sink of evergreen forests under continuously increasing N deposition, because more than 40% of the total canopy biomass of evergreen species is made up by foliage older than one year (Sala, 1992, Li et al. 2006, Yang et al. 2021). It has been suggested that the N allocated and thus

the photosynthetic rates inherently decline with leaf aging (Zhou et al., 2015; Li et al., 2017), implying a stronger photosynthetic response of younger foliage than older foliage to N deposition, so that they can obtain an optimal C gain (Niinemets, 2007). This indicates that the N saturation threshold for productivity is determined more by younger foliage than by older foliage. However, plants under N deposition might be able to invest more N to older foliage, thereby mitigating the difference in photosynthetic response to N addition and thus the contribution to the N saturation threshold for productivity among needle age classes. These speculations still awaits experimental test.

Chinese fir (*Cunninghamia lanceolata* (Lamb.) Hook.), which is native to and mainly distributed in the subtropical China, has the largest area of forest plantation in China (State Forestry Administration of China, 2018). Nevertheless, there still lacks the detail information about how C uptake capacity of this species would respond to N amendment. In this study, effects of N addition rates on aboveground net primary productivity (ANPP) of young Chinese fir trees were estimated. Further, we linked the ANPP to the photosynthetic parameters, to understand the physiological mechanisms that determine the response of C uptake to N deposition. We hypothesized that (i) the response of both photosynthesis and ANPP to increasing N addition rate is nonlinear, with positive fertilization effects at lower N addition rates and remain a stable at higher N addition rates; (ii) both needle $\delta^{13}C$ and $\delta^{18}O$ increase after N addition, as a result of photosynthetic capacity increase and stomatal conductance decrease following N addition; and (iii) the photosynthesis of both young and old needles

account for the response of the ANPP to N addition.

2 Materials and methods

2.1. Study site and experimental design

The experiment was carried out in the Huitong National Research Station of Forest Ecosystem (26°50′ N, 109°36′ E) in Hunan Province, Southern China. This region is located at subtropical zone, with an annual precipitation of 1200 mm and an annual temperature of 16.5 °C on average (Li et al., 2017). The elevation here is about 280 m above sea level. The soil type according to the World Reference Base for Soil Taxonomy is haplic alisols.

The experiment was conducted in a custom-built Ecological-Process-Experiment platform, on which thirty independent plots was constructed of concrete (Fig. 1). Each of the plots had a size of 1 m in length×1 m in width×1 m in depth, with a drain hole in its bottom. In September 2017, these plots were filled with soil collected from the surface layer (0-20cm) of a nearby Chinese fir plantation after it was thoroughly mixed. In March 2018, after stabilization for 6 months, the one-year old Chinese fir seedlings selected from a local nursery with similar plant height, basal diameter and fresh weight were planted in the plots (one tree per plot). This platform avoids errors from soil heterogeneity, thereby allowing us to more accurately estimate the response of tree physiology to N deposition. After three treatment years when the physiological traits were assessed in July 2020, those trees had a mean diameter at breast height (DBH) of about 3.8 cm and a mean height (H) of about 3.1m.

The experimental design obeyed a completely random design, which contained

five N addition levels with six replicates. Specifically, the N dose for each treatment was arranged as follows: control treatment without N addition; 5.6 g N m^{-2} yr^{-1}; 11.2 g N m^{-2} yr^{-1}; 22.4 g N m^{-2} yr^{-1}; 44.8 g N m^{-2} yr^{-1}. The N input, which was begun at the second month (i.e. April 2018) after planting those trees, was applied in solution form with 12 times every year at monthly interval. At each N application, targeted amount of NH_4NO_3 fertilizer was weighed, mixed with 1 L of water, and sprayed onto the floor of N-treated plots evenly. 1 L of water without NH_4NO_3 fertilizer was evenly sprayed onto the floor of control plots. The amount of solution or water added per year represents 12 mm in precipitation.

2.2 ANPP estimation

The DBH and H were measured for each tree in each plot in July 2019 and July 2020, respectively (Table 1). ANPP was defined as the difference of aboveground biomass between July 2019 and July 2020. The total biomass (B) of aboveground organs (needles, branches, stem wood, and stem bark) was estimated using an allometric equation (Wang et al., 2010):

$$\mathrm{B} = 25.59(DBH^2\mathrm{H}) + 519$$

the units for B, DBH, and H are gram, centimeter, and metre, respectively. This allometric equation was established based on young Chinese fir trees that grown in the plots near our study site. Those trees had a mean DBH of 3.6 cm (ranged from 2.3 to 5.6 cm) and a mean H of 3.6 m (ranged from 2.5 to 5.3 m), thus was comparable with the tree sizes in our study. The increase in N availability may alter tree allometric relationships, thus using an allometric equation gain in ambient situation to estimating

the biomass of N-treated trees likely bring some bias. However, Ibáñez et al. (2016) reported that N amendment mostly changes the allometric relationship of aboveground part of large (with a DBH of ＞ 20cm) rather than small trees. Therefore, this allometric equation should be effective in representing the aboveground biomass in this study.

2.3 Gas exchange measurement

Gas exchange was measured during July 25 to July 30, 2020, using a portable photosynthesis system with a red/blue LED light source and a CO_2 injector (LI-6400, LI-COR, Inc., Lincoln, NE, USA). Measurement was implemented on current- and one-year needles from the middle section of the canopy were conducted between 9:00 and 11:00 am at each sampling date. When measuring, light intensity and CO_2 concentration in the leaf chamber were set to 1500 μmol m^{-2} s^{-1} and 400 ppm, respectively. Leaf temperature was kept at about 25 °C, and the needle-to-air vapor pressure deficit was in the scope of 0.75 mmol mol^{-1} to 1.5 mmol mol^{-1}. Before recording the photosynthetic rates, needles were allowed to acclimate to the light intensity for 5–15 min until stable values were appeared. Afterwards, the needles enclosed in the chamber were collected and scanned using a leaf area meter (LI-3000, LI-COR, Inc., Lincoln, NE, USA), by which the photosynthetic rates were corrected to the actual leaf area.

2.4 Needle chemistry determination

Approximately 40–50 needles of each needle class, which was near the needles used for photosynthetic assessment, were collected immediately after photosynthetic

measurements and divided into two portions. One portion, which was used for the assessment of the concentrations of C and oxygen (O) isotopes, total N, magnesium (Mg), potassium (K), and phosphorus (P) was oven-dried at 65 °C until a constant mass, before it was ground in a ball mill and passed through a 0.2 mm mesh sieve. The other portion was for water-soluble N measurement was immediately stored in a liquid nitrogen tank.

Isotopes (^{13}C and ^{18}O) from needle cellulose were measured, because cellulose is immobile within needles once it has been deposited within the cell walls (McDowell et al., 2003). The extraction of needle cellulose followed the method described by Leavitt and Danzer (1993). Afterwards, about 2 mg of extracted needle cellulose was weighed, combusted to CO_2 or pyrolized to CO under high-temperature using an elemental analyzer (Flash 2000HT, Thermo Fisher Scientific, Inc., USA). The produced CO_2 and CO were analyzed with a coupled isotope ratio mass spectrometer (Finnigan Delta V Advantage, Thermo Fisher Scientific, Inc., USA) to determine $\delta^{13}C$ and $\delta^{18}O$, respectively. The $\delta^{13}C$ and $\delta^{18}O$ composition (‰) were referenced relative to the Vienna Pee Dee Belnite (VPDB) and Vienna Standard mean Ocean Water (VSMOW), respectively, and expressed as follows:

$$\delta^{13}\mathrm{C} \text{ or } \delta^{18}O = \left(\frac{R_{sample}}{R_{standard}} - 1\right) \times 1000$$

The total N of needle was assessed by a Vario MAX CN analyzer (Elementar Analysensysteme GmbH, Hanau, Germany). The concentrations of needle Mg, K, and P were determined as described by Dong (1996). In brief, 1 g of needle subsamples were digested with 15 ml HNO_3 and $HClO_4$ (5 : 1 in volume ratio) solution.

Subsequently, the P concentration was measured by a continuous flow injection analyzer (AA3, Seal, Germany), and the Mg and K concentration were assessed by an atomic absorption spectrometer (AA240, Varian, America).

The concentration of water-soluble N was determined as described by Li et al. (2020 b). Briefly, about 2 g frozen samples were ground in liquid nitrogen in a mortar with a pestle and transferred to a centrifuge tube by using 10 ml of 100 mM sodium phosphate buffer (pH 7.5) containing 0.4 M sorbitol, 10 mM NaCl, 2 mM $MgCl_2$, 5 mM iodoacetate, 5 mM dithiothreitol, 5 mM phenylmethylsulfonyl fluoride and 1% (v/v) polyvinylpyrrolidone. Then, the homogenate was centrifuged at 15000 × g for 30 min, and the supernatants were collected, before it was precipitated with 10% trichloroacetic acid. Subsequently, the precipitate was hydrolyzed in an autoclave (120 °C, 0.12 MPa) with 0.316 mM $Ba(OH)_2$ for 15 min. After hydrolysis, the protein content was determined by the ninhydrin method (McGrath, 1972). To calculate the water-soluble N content from the soluble protein fractions, a conversion coefficient of 0.16 g N g^{-1} protein was used (Hikosaka and Terashima, 1996).

2.5 Soil property determination

Volumetric soil moisture was measured approximately once a month from August 2018 to July 2020 by the probes attached to an LI-8100 automated soil CO_2 flux system (LI-COR Inc., Lincoln, NE, USA). Soil samples were collected in July 2020 for pH, N, and exchangeable cations analysis. Three soil cores (5 cm in diameter and 20 cm in depth) were randomly collected from each plot and bulked into a composite sample. These soil samples were sieved with a 2 mm mesh sieve to remove stones and

roots. Soil pH was measured using a pH meter in a 1:2.5 mixture of soil and deionized H_2O. Soil total N was assessed by the Vario MAX CN analyzer. Soil NH_4^+ and NO_3^- were measured by the continuous flow injection analyzer after extraction with 2M KCl. The exchangeable K^+ and Mg^{2+} were extracted with 1 M ammonium acetate, and then analyzed by the atomic absorption spectrometer (Lu, 1999).

2.6 Statistical analysis

A quadratic-plus-plateau model which is defined by the following equations was used to fit the relationship between ANPP and N rate (Peng et al., 2020):

$$\mathrm{ANPP} = \mathrm{a}x^2 + \mathrm{b}x + \mathrm{c}, \mathrm{if}\ \ \mathrm{x} \leq \mathrm{d}$$

$$\mathrm{ANPP} = \mathrm{P}, \mathrm{if}\ \ \mathrm{x} > \mathrm{d}$$

where x is N addition rate (g N m^{-2} $year^{-1}$); a, b, c, d, and P are the parameters of this model. All parameters were determined using the Gauss–Newton iterative algorithm to minimize the residual sum of squares. Here, the constant d means the N rate where the ANPP variation changes from an increasing stage to a plateaued pattern with continuously N input. In the plateaued stage, ANPP achieved the maximum value-P.

Linear mixed effect model was used to test the effect of N addition, needle age, and their interaction on the net photosynthetic rates, stomatal conductance, and the concentrations of total N, water-soluble N, K, Mg, P, $\delta^{13}C$ and $\delta^{18}O$ of needles. In this model, N addition and needle age were considered as fixed effects, and the plot was assigned as random effect. Fisher's Least Significant Difference (LSD) was performed as a post hoc test to separate differences among treatments once the main effect was significant ($P < 0.05$) or marginally significant ($P < 0.10$). The effect

of N addition on soil water content, NH_4^+, NO_3^-, pH value, K^+ and Mg^{2+} was assessed by one-way analysis of variance (ANOVA), followed by a post hoc test using LSD. Linear regression analyses were used to determine the relationship between ANPP and net photosynthetic rates, as well as net photosynthetic rates and needle total N and water-soluble N content. All the statistics were conducted in the R programming language (R Development Core Team 2008).

3 Results

3.1 ANPP and photosynthetic rate

The quadratic-plus-plateau model was effective in fitting the relationship between N rates and ANPP (Fig. 2). Results showed that ANPP first increased with N addition rates and then changed to a plateaued stage at an N rate of 16.3 g m^{-2} yr^{-1} (Fig. 2). Similar to ANPP, needle area-based photosynthetic rates also showed a significant (P = 0.001) and nonlinear enhancement in response to N addition (Appendix, Table S1; Fig. 3 a). We found a marginally significant (P = 0.063) interaction between N treatment and needle age, indicating that N addition increased the photosynthetic rates of the current-year but not the one-year old needles (Appendix, Table S1; Fig. 3 a). The ANPP was found to be significantly positively correlated with the area-based photosynthetic rates of the current-year needles (P = 0.001) but not with that of one-year old needles ($P > 0.10$) (Fig. 3 b).

3.2 Needle $\delta^{13}C$ and $\delta^{18}O$

The N addition significantly (P = 0.001) increased needle $\delta^{13}C$ (Appendix, Table S2; Fig. 4 a). The needle $\delta^{13}C$ value increased dramatically when N addition rate

increased from 0 to 11.2 g m^{-2} yr^{-1}, and kept constant under further N addition rate that continuously increased to 44.8 g m^{-2} yr^{-1}, showing a non-linear response (Fig. 4 a). No interaction between N rates and needle age was found on needle $\delta^{13}C$ (Appendix, Table S2). Unlike needle $\delta^{13}C$, needle $\delta^{18}O$ of both the current-year and one-year old needles did not respond to N addition (Appendix, Table S2; Fig. 4 b).

3.3 Needle traits

Stomatal conductance did not respond to N addition (Appendix, Table S3; Fig. 5 a). Needle total N content increased continuously with increasing N addition rate (Appendix, Table S3; Fig. 5 b). The needle water-soluble N content increased when N addition rate increased from 0 to 11.2 g m^{-2} yr^{-1}, and then the increase diminished when N addition rate continuously increased to 44.8 g m^{-2} yr^{-1} (Appendix, Table S3; Fig. 5 c). A significant interaction between N rates and needle age was detected, showing stronger effects of N addition on needle water-soluble N content in current-year than in one-year old needles (Appendix, Table S3; Fig. 5 c). Moreover, needle Mg and K concentrations declined with N addition (Appendix, Table S3; Fig. 5 d and e), and needle P concentration did not respond to N addition (Appendix, Table S3; Fig. 5 f).

Total N content of current-year needles was significantly positively correlated with net photosynthetic rates (R^2 = 0.316; P = 0.001) (Fig. 6 a). However, net photosynthetic rates of the one-year old needles could not be explained ($P > 0.10$) by the variations in needle total N content (Fig. 6 a). Water-soluble N content had significant positive relationship with net photosynthetic rates of both current-year (R^2

= 0.666; $P < 0.001$) and one-year old needles ($R^2 = 0.160$; $P = 0.029$) (Fig. 6 b).

3.4 Soil properties

Overall, soil moisture, especially those under 22.4 and 44.8 g N m^{-2} yr^{-1}, decreased significantly with N addition (Fig. 7 a). Soil NH_4^+-N and NO_3^--N generally increased with N addition (Fig. 7 b and c). Compared to the control treatment, N input ranging from 5.6 to 22.4 g m^{-2} yr^{-1} had negligible influence on soil pH, but N addition at the rate of 44.8 g m^{-2} yr^{-1} led to significant lower soil pH (Fig. 7 d). Similar to soil pH, 44.8 g N m^{-2} yr^{-1} rather than other N addition rates markedly decreased the concentrations of soil K^+ and Mg^{2+} (Fig. 7 e and f).

4 Discussion

4.1 Photosynthetic response to N addition

In the present study, an enhanced net photosynthetic rate after N addition was found, which agrees with some previous studies that N deposition had a fertilization effect on plants (Guo et al., 2016; Li et al., 2016; Duan and Chang, 2017). With increasing N addition, the photosynthetic rate increased rapidly until the N rate of 11.2 g m^{-2} yr^{-1}, and thereafter it did not change under further N addition, although the needle N content continuously increased. This result was in line with our first hypothesis, and it seems that an additional N input beyond 11.2 g m^{-2} yr^{-1} may exceed the biotic N demand and induce N saturation for these young Chinese fir trees.

Like the net photosynthetic rate, needle $\delta^{13}C$ also increased nonlinearly in relation to N application, indicating different responses of stomatal conductance or photosynthetic capacity or both to N addition below and above the saturation

threshold (Farquhar et al., 1982). However, needle $\delta^{18}O$ remained unchanged across the N treatment gradient, demonstrating that stomatal conductance was not a factor that mediated the photosynthetic response to N addition (Scheidegger et al., 2000). It's important to note that the use of the conceptual model of Scheidegger et al. (2000) requires a same ^{18}O signature of the source water and of the atmospheric water vapour among the target trees. In this study, trees were planted in homogeneous soil within a small scale, thus they avoided deviations of $\delta\ ^{18}O$ from source water and atmospheric water vapour. We thus concluded that the increased needle $\delta^{13}C$ after N addition was a result of the enhancement in photosynthetic capacity. These findings only support partially our second hypothesis.

The unresponsive stomatal conductance measured as needle $\delta^{18}O$ was in consistent with the instantaneous measurement of gas exchange. Interestingly, we have detected a significant decrease in soil moisture in response to N addition. In a subtropical moist forest, Li et al. (2015) also found that soil moisture decreased significantly with N addition. The reason responsible for the unaltered stomatal conductance following N addition might be that water in the subtropical ecosystem is not a limiting factor for plant growth (Li et al., 2017), thus the significant but slight soil water decline should have not triggered water shortage for those N-treated trees. Our findings suggested that N deposition would not impose a water stress to this species, which distributed mainly in the rain-rich subtropical regions in China.

Our results implied that the photosynthetic capacity of needle increased nonlinearly with increasing N addition. N is generally a limiting resource for plants

(Bai et al., 2010). With increasing N addition rate up to the threshold of N saturation, trees' demand for N is progressively satisfied, by which they are able to invest more N to photosynthetic apparatus to strengthen photosynthetic capacity and obtain an optimal C gain (Niinemets, 2007). This interpretation was reinforced by the increasing needle water-soluble N concentration when N addition rate increased from 0 to 11.2 g m^{-2} yr^{-1}. Water-soluble N was used to represent N that involved in photosynthesis in this study, because CO_2-fixing enzymes are associated mainly with water-soluble fraction rather than other components of total N (Li et al., 2020). Consistently, the variation in photosynthetic rates was more explained by water-soluble N than by total N.

Beyond the N saturation threshold, other nutrients may become to limit plant growth due to nutrient imbalance (Arens et al., 2008). Along with N, nutrients like P and other cations are also necessary for healthy plant, and the shortage of those nutrients is assumed to constrain foliar photosynthesis by suppressing N partitioning to photosynthetic apparatus (Warren and Adams 2002; Guo et al., 2016; Mao et al., 2018). In our study, nutrients like P, Mg, and K in needles were either constant or decreased with N addition, leading to increasing ratios of N to these nutrients. There are two potential mechanisms for the reduced needle Mg and K concentration: one being that soil acidification resulted from N addition has triggered base cations leaching; and the other is that decreased root uptake of cations may arise from ion competition with NH_4^+ (Liang et al., 2020; Mao et al., 2018). Both the two mechanisms were possible, because soil pH value decreased and NH_4^+ concentration

increased with N addition rates in the present study. When reaching the N saturation threshold, the raising nutrient imbalance caused by continuously increased N accumulation and the relative shortage of other nutrients exceeds tree tolerance, which might inhibit greater use of N by photosynthetic apparatus. This interpretation was well supported by the fact that no additional increase in water-soluble N occurred when N addition rate was above 11.2 g m^{-2} yr^{-1}.

4.2 Effect of N addition on ANPP

The ANPP increased rapidly to the N saturation threshold, and thereafter it kept the similar respond to further N addition. We found that the variation in ANPP was well explained by the net photosynthetic rates. Low N addition favored the ANPP through enhancing the net photosynthetic rate, while N addition above the saturation threshold inhibited the continuous increase of ANPP, because it failed to continue increasing the net photosynthetic rate. In addition to needle net photosynthetic rate, total area of the foliage might also increase following N addition, which can be another mechanism whereby the Chinese fir trees achieve increased ANPP after N addition (Wang et al., 2017). Unfortunately, this mechanism was not quantified in the present study, because the proportional biomass/area of current- and 1-year old needles was not determined.

In this study, the N saturation threshold for ANPP was 16.3 g N m^{-2} yr^{-1}, which is clearly higher than that in Wei et al. (2012), who published an N saturation threshold for Chinese fir plantations of 2-3 g N m^{-2} yr^{-1}. Except for the different models used in the two studies, this discrepancy might also be ascribed to the differences in stand age. Trees older than 15 years were included in the experiment of Wei et al. (2012), and

those mature trees with decreased growth potential likely have a lower demand for N, thus were easily to be saturated by N addition (Ibáñez et al., 2016). These results indicate that stand age of forests affects the N saturation threshold. Thus, our study provided an experimental footing for evaluating C sink of young Chinese fir plantation in the context of continuously increasing N deposition. In the main distribution area of Chinese fir in subtropical China, N deposition is now between 1.5 to 3 g N m^{-2} $year^{-1}$, with average rates of increase of about 0.05 g N m^{-2} $year^{-1}$ (Yu et al., 2019; Liu et al., 2013). A survey by the government showed that up to 40% of the area of Chinese fir plantation was occupied by young trees (State Forestry Administration of China, 2018). Thus, the overall C sink of this species is expected benefit from N deposition.

No supports were found for our third hypothesis, because the ANPP-N relationship was determined by the photosynthesis of the current-year needles rather than that of the one-year old needles. Recently, Yang et al. (2021) also experimentally found that older needles of *Abies alba* trees did not significantly contribute to height and diameter growth. Our result should be a consequence of the fact that N addition exerted more obvious effect on photosynthesis of the current-year needles than that of the one-year old needles, which might be interpreted as follows. First, more obtained N was allocated to younger needles. However, this interpretation did not work well given total N content in the current-year needles was not higher than that in the one-year old needles. Second, more N in the current-year needles was used for photosynthesis. For an evergreen species, older foliage is gradually shaded by newly

growing ones, and as a result, it is often light limited (Li et al., 2017). The light deficiency might impede needle N partitioning to water-soluble fraction (Dong et al., 2015), and further reduce the sensitivity of photosynthesis to N addition. In agreement with this explanation, water-soluble N concentration in our study was lower in one-year than in current-year needles.

4.3 Study limitations

Although our work advances the understanding on how the productivity of Chinese fir plantations would respond to aggravating N deposition, we also admit that this study has some limitations. First, our study lasted for a relative short time (29 months). Previous study has reported that the response of plant growth to N addition decreased over time, because the increased soil N would promote the transformation of inorganic P to the organic state progressively and cause P limitation for plants (Schleuss et al., 2020), which might adjust the N saturation threshold. In this case, further investigations that explore whether the conclusions in this study fit also the chronic situation might be necessary. Second, each tree was planted in a separate plot, thus the possible effect of intraspecific competition on the N saturation threshold was ignored. Recent study has revealed that the intraspecific competition within Chinese fir trees could decrease net soil N mineralization by reducing rhizosphere priming effects (Yin et al., 2018). As such, although our experiment can provide homogeneous soil to each tree, thus avoid errors from soil heterogeneity in evaluating the response of tree physiology, it might have a risk to underestimate the N saturation threshold. Third, only mineral soil from surface soil layer was used in our study, which has

eliminated the soil horizons. This might cause a bias in estimating the N saturation threshold of real forest ecosystems that have complete soil horizons, because the traits of natural soil generally vary with its depth (Pang et al., 2015).

5 Conclusion

The present study indicates that the needle photosynthetic C gain and ANPP of Chinese fir trees will increase in response to increasing N deposition, revealed by instantaneous gas exchange and time-integrating isotopes. However, we found that the increase in ANPP with increasing N addition rate stopped at an N saturation threshold of 16.3 g N m^{-2} $year^{-1}$, beyond which further N addition did not affect photosynthesis and ANPP, probably due to shortage of other nutrients. We found that variation in photosynthetic capacity rather than needle stomatal conductance determined the nonlinear response of photosynthesis and thus ANPP to N addition. Moreover, net photosynthetic rate of the younger needles was more effective than that of the older needles in predicting the trends of ANPP following N deposition. Considering the present and the predicted N deposition in subtropical China, we expect that the C sink of the Chinese fir plantations widely distributed in southern China would generally benefit from future N deposition.

Acknowledgements

This work was supported by the National Natural Science Foundation of China (Grant Nos. 41877092, 32192434, U1805243). We also thank Xiuyong Zhang, Zhenqi Shen, Xiaojun Yu, Ke Huang, and Munan Zhu for their invaluable assistance in the laboratory and the field experiments.

References

Aber, J.D., Nadelhoffer, K.J., Steudler, P., Melillo, J.M., 1989. Nitrogen saturation in northern forest ecosystems. *BioScience* 39, 378- 386.

Aber, J., McDowell, W., Nadelhoffer, K., Magill, A., Berntson, G., Kamakea, M. et al., 1998. Nitrogen saturation in temperate forest ecosystems – hypotheses revisited. *Bioscience* 48, 921–934.

Arens, S.J.T., Sullivan, P.F., Welker, J.M., 2008. Nonlinear responses to nitrogen and strong interactions with nitrogen and phosphorus additions drastically alter the structure and function of a high arctic ecosystem. *Journal of Geophysical Research: Biogeosciences* 113, G03S09.

Bai, Y., Wu, J., Clark, C.M., Naeem, S., Pan, Q., Huang, J. et al., 2010. Tradeoffs and thresholds in the effects of nitrogen addition on biodiversity and ecosystem functioning: evidence from inner Mongolia Grasslands. *Global Change Biol*. 16, 358–372.

Bauer, G.A., Berntson, G.M., Bazzaz, F.A., 2001. Regenerating temperate forests under elevated CO_2 and nitrogen deposition: comparing biochemical and stomatal limitation of photosynthesis. *New Phytol*. 152, 249–266.

Bauer, G.A., Bazzaz, F.A., Minocha, R., Long, S., Magill, A., Aber, J., Berntson, G.M., 2004. Effects of chronic N additions on tissue chemistry, photosynthetic capacity, and carbon sequestration potential of a red pine (*Pinus resinosa* Ait.) stand in the NE United States. *Forest Ecol. Manag.* 196, 173–186.

de Vries, W., Du, E., Butterbach-Bahl, K., 2014. Short and long-term impacts of nitrogen deposition on carbon sequestration by forest ecosystems. *Curr. Opin. Env. Sust. 9–10*, 90–104.

Dong M., 1996. Survey, observation and analysis of terrestrial biocommunities [In Chinese].

Standards Press of China, Beijing.

Dong, T.F., Li, J.Y., Zhang, Y.B., Korpelainen, H., Niinemets, Ü., Li, C.Y., 2015. Partial shading of lateral branches affects growth, and foliage nitrogen- and water-use efficiencies in the conifer *Cunninghamia lanceolata* growing in a warm monsoon climate. *Tree Physiol.* 35, 632–643.

Duan, M., Chang, S.X., 2017. Nitrogen fertilization improves the growth of lodgepole pine and white spruce seedlings under low salt stress through enhancing photosynthesis and plant nutrition. *Forest Ecol. Manag.* 404, 197–204.

Farquhar, G.D., O'Leary, M.H., Berry, J.A., 1982. On the relationship between carbon isotope discrimination and intercellular carbon dioxide concentration in leaves. *Aust. J. Plant Physiol.* 9, 121–137.

Farquhar, G.D., Ehleringer, J.E., Hubick, K., 1989. Carbon isotope fractionation and photosynthesis. Annu. Rev. Plant Physiol. *Plant Mol. Biol.* 40, 503–537.

Farquhar, G.D., Cernusak, L.A., Barnes, B., 2007. Heavy water fractionation during transpiration. *Plant Physiol.* 143, 11–18.

Giuggiola, A., Ogée, J., Rigling, A., Gessler, A., Bugmann, H., Treydte, K., 2016. Improvement of water and light availability after thinning at axeric site: which matters more? A dual isotope approach. *New Phytol.* 210, 108–121.

Guo, J., Wu, Y.Q., Wang, B., Lu, Y., Cao, F.L., Wang, G.B., 2016. The Effects of Fertilization on the Growth and Physiological Characteristics of Ginkgo biloba L. *Forests* 7, 293.

Hikosaka, K., Terashima, I., 1996. Nitrogen partitioning among photosynthetic components and its consequence in sun and shade plants. *Funct. Ecol.* 10, 335–343.

Hu, Y.T., Schäfer, K.V.R., Zhu, L.W. et al., 2021. Impacts of canopy and understory nitrogen

additions on stomatal conductance and carbon assimilation of dominant tree species in a temperate broadleaved deciduous forest. *Ecosystems*, doi.org/10.1007/s10021-020-00595-4

Högberg, P., 2007. Nitrogen impacts on forest carbon. *Nature* 447, 781–782.

Ibáñez, I., Zak, D.R., Burton, A.J., Pregitzer, K.S., 2016. Chronic nitrogen deposition alters tree allometric relationships: implications for biomass production and carbon storage. *Ecol. Appl.* 26, 913–925.

Krause, K., Cherubini, P., Bugmann, H., Schleppi, P., 2012. Growth enhancement of Picea abies trees under long-term, low-dose N addition is due to morphological more than to physiological changes. *Tree Physiol*. 32, 1471–1481.

King, N.T., Seiler, J.R., Fox, T.R., Johnsen, K.H., 2008. Post-fertilization physiology and growth performance of loblolly pine clones. *Tree Physiol*. 28, 703–711.

Leavitt, S.W., Danzer, S.R., 1993. Methods for batch processing small wood samples to holocellulose for stable-carbon isotope analysis. *Anal. Chem.* 65, 87–89.

Li, R.H., Zhu, S.D., Chen, S.Y.H., John, R., Zhou, G.Y., Zhang, D.Q., Zhang, Q.M., Ye, Q., 2015. Are functional traits a good predictor of global change impacts on tree species abundance dynamics in a subtropical forest? Ecol. Lett. 18, 1181–1189.

Li, J.Y., Guo, Q.X., Zhang J.X., Korpelainen, H., Li, C.Y., 2016. Effects of nitrogen and phosphorus supply on growth and physiological traits of two *Larix* species. *Environ. Exp. Bot*. 130, 206–215.

Li, M.H., Kräuchi, N., Dobbertin, M., 2006. Biomass distribution of different-aged needles in young and old *Pinus cembra* trees at highland and lowland sites. Trees 20: 611-618.

Li, R.S., Yang, Q.P., Zhang, W.D., Zheng, W.H., Chi, Y.G., Xu, M., Fang, Y.T., Gessler, A., Li,

M.H., Wang, S.L., 2017. Thinning effect on photosynthesis depends on needle ages in a Chinese fir (Cunninghamia lanceolata) plantation. *Sci. Total Environ*. 580, 900–906.

Li, Y.Q., Zhao, P., Zhang, Z.Z., Zhu, L.W., Ouyang, L., Ni, G.Y., 2020 a. Inconsistent Responses of Transpiration of Different Canopy Layers to Simulated Canopy and Understory N Depositions in a Low‐Subtropical Evergreen Broadleaf Forest. *JGR: Biogeosciences* 125, e2019JG005594.

Li, R.S., Han, J.M., Guan, X., Chi, Y.G., Zhang, W.D., Chen, L.C., Wang, Q.K., Xu, M., Yang, Q.P., Wang, S.L., 2020 b. Crown pruning and understory removal did not change the tree growth rate in a Chinese fir (*Cunninghamia lanceolata*) plantation. *Forest Ecol. Manag.* 464, 118056.

Li, Z.L., Zeng, Z.Q., Song, Z.P., Wang, F.Q., Tian, D.S., Mi, W.H., Huang, X., Wang, J.S., Song, L., Yang, Z.K., Wang, J., Feng, H.J., Jiang, L.F., Chen, Y., Luo, Y.Q., Niu, S.L., 2021. Vital roles of soil microbes in driving terrestrial nitrogen immobilization. *Glob Change Biol.* 27, 1848–1858.

Liu, X., Zhang, Y., Han, W., Tang, A., Shen, J., Cui, Z., et al., 2013. Enhanced nitrogen deposition over China. *Nature* 494, 459–462.

Lu, R.K., 1999. Analytic methods of soil and agriculture chemistry [In Chinese]. China agricultural science and technology press, Beijing.

Lu, X.K., Vitousek, P.M., Mao, Q.G., Gilliam, F.S., Luo, Y.Q., Zhou, G.Y., Zou, X.M., Bai, E., Scanlon, T.M., Hou, E.Q., Mo, J.M., 2018. Plant acclimation to long-term high nitrogen deposition in an N-rich tropical forest. *Proc. Natl. Acad. Sci. USA* 115, 5187–5192.

Liang, X.Y., Zhang, T., Lu, X.K. et al., 2020. Global response patterns of plant photosynthesis to nitrogen addition: A meta-analysis. *Glob Change Biol*. 26, 3585–3600.

Mao, Q.G., Lu, X.K., Mo, H., Gundersen, P., Mo, J.M., 2018. Effects of simulated N deposition on foliar nutrient status, N metabolism and photosynthetic capacity of three dominant understory

plant species in a mature tropical forest. *Sci Total Environ*. 610–611:555–562.

McDowell, N.G., Brooks, J.R., Fitzgerald, S.A., Bond, B.J., 2003. Carbon isotope discrimination and growth response of old Pinus ponderosa trees to stand density reductions. *Plant Cell Environ.* 26, 631–644.

McGrath, R., 1972. Protein measurement by ninhydrin determination of amino acids released by alkaline hydrolysis. *Anal. Biochem.* 49, 95–102.

Niinemets, Ü., 2007. Photosynthesis and resource distribution through plant canopies. *Plant Cell Environ.* 30, 1052–1071.

Pang, X.Y., Zhu, B., Lv, X.T., Cheng, W.X., 2015. Labile substrate availability controls temperature sensitivity of organic carbon decomposition at different soil depths. *Biogeochemistry* 126, 85–98.

Peng, Y.F., Chen, H.Y.H., Yang, Y.H., 2020. Global pattern and drivers of nitrogen saturation threshold of grassland productivity. *Funct. Ecol.* 34, 1979–1990.

Sala, A., 1992.Water Relations, Canopy Structure, and Canopy Gas Exchange in a Quercus ilex Forest: Variation in Time and Space. Ph.D. Thesis, Universitat de Barcelona, Barcelona.

Scheidegger, Y., Saurer, M., Bahn, M., Siegwolf, R., 2000. Linking stable oxygen and carbon isotopes with stomatal conductance and photosynthetic capacity: a conceptual model. *Oecologia* 125, 350–357.

Schleuss, P. M., Widdig, M., Heintz-Buschart, A., Kirkman, K., Spohn, M., 2020. Interactions of nitrogen and phosphorus cycling promote P acquisition and explain synergistic plant-growth responses. *Ecology* 101, e03003.

State Forestry Administration of China, 2018. Forest Resources Report in China (2014–2018).

China Forestry Publishing House, Beijing.

Tian, D.S., Niu, S.L., Pan, Q.M., Ren, T.T., Chen, S.P., Bai, Y.F., Han, X.G., 2016. Nonlinear responses of ecosystem carbon fluxes and water-use efficiency to nitrogen addition in Inner Mongolia grassland. *Funct. Ecol.* 30, 490–499.

Talhelm, A.F., Pregitzer, K.S., Burton, A.J., 2011. No evidence that chronic nitrogen additions increase photosynthesis in mature sugar maple forests. *Ecol. Appl.* 21, 2413–2424.

Vitousek, P.M., Aber, J.D., Howarth, R.W., Likens, G.E., Matson, P.A., Schindler, D.W., Schlesinger, W.H., Tilman, D., 1997. Human alteration of the global nitrogen cycle: Sources and consequences. *Ecol. Appl.* 7, 737–750.

Wang, M., Zhang, W.W., Li, N., Liu, Y.Y., Zheng, X.B., Hao, G.Y., 2017. Photosynthesis and growth responses of *Fraxinus mandshurica* Rupr. seedlings to a gradient of simulated nitrogen deposition. *Ann. Forest Sci*. 75:1

Wang, S.L., Zhang, W.D., Sanchez, F., 2010. Relating net primary productivity to soil organic matter decomposition rates in pure and mixed Chinese fir plantations. *Plant Soil* 334, 501–510.

Warren CR, Adams MA (2002) Phosphorus affects growth and partitioning of nitrogen to Rubisco in *Pinus pinaster*. *Tree Physiol.* **22**, 11–19.

Wei, X.H., Blanco, J.A., Jiang, H., Kimmins, J.P.H., 2012. Effects of nitrogen deposition on carbon sequestration in Chinese fir forest ecosystems. *Sci Total Environ*. 416, 351–361

Yang, Y., Wang, A., Cherubini, P., Kräuchi, N., Ni, Y., Wu, Z., He SH, Li, MH, Schaub, M., 2021. Physiological and growth responses to defoliation of older needles in *Abies alba* trees grown under two light regimes. *Forest Ecol. Manag.* 484, 118947.

Yin, L.M., Dijkstra, F.A., Wang, P., Zhu, B., Cheng, W.X., 2018. Rhizosphere priming effects on

soil carbon and nitrogen dynamics among tree species with and without intraspecific competition. *New Phytol*. 218, 1036–1048.

Yu, G.R., Jia, Y.L., He, N.P. et al., 2019. Stabilization of atmospheric nitrogen deposition in China over the past decade. *Nat. geosci*. 12, 424–429.

Zhou, H.R., Xu, M., Pan, H.L., Yu, X.B., 2015. Leaf-age effects on temperature responses of photosynthesis and respiration of an alpine oak, *Quercus aquifolioides*, in southwestern China. *Tree Physiol.* 35, 1236–1248.

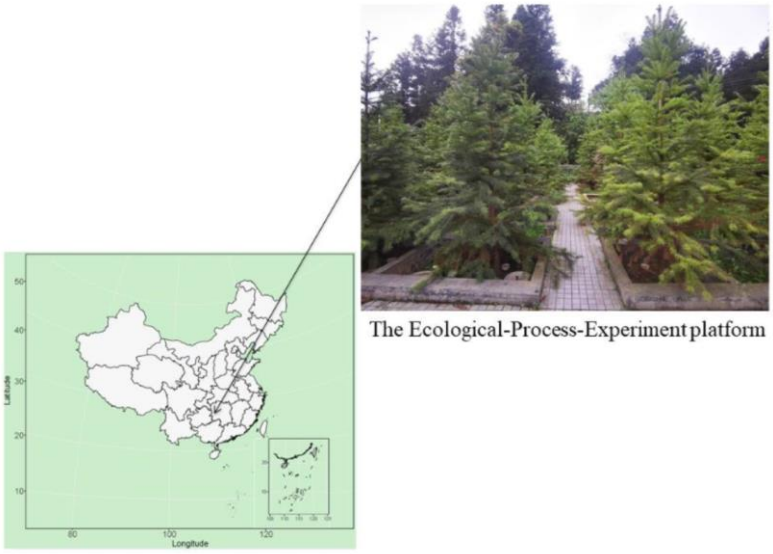

Fig. 1 Location of the Ecological-Process-Experiment platform

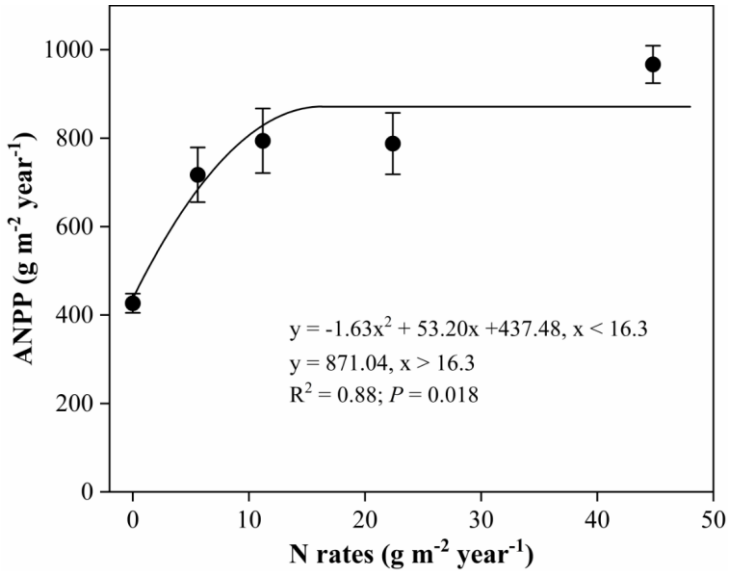

Fig. 2 The quadratic-plus-plateau relation between above-ground net primary productivity (ANPP) and N addition rates. Values are means ± SE (n = 6).

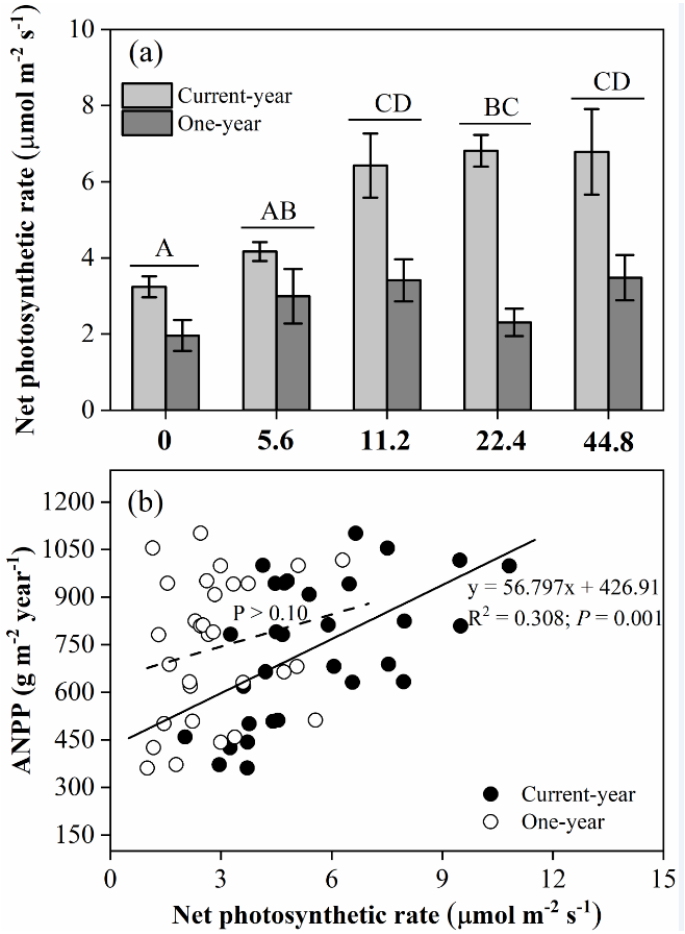

Fig. 3 Variations of needle area-based light-saturated net photosynthetic rate of current- and one-year old needles with different N addition rates (g N m^{-2} yr^{-1}) (a). Values are means ± SE (n =

6). Different capital letters indicated significant differences among N treatments based on the results of mixed effect model shown in Table S1. The subplot (b) showed the relationship between ANPP and net photosynthetic rates of current- or one-year old needles.

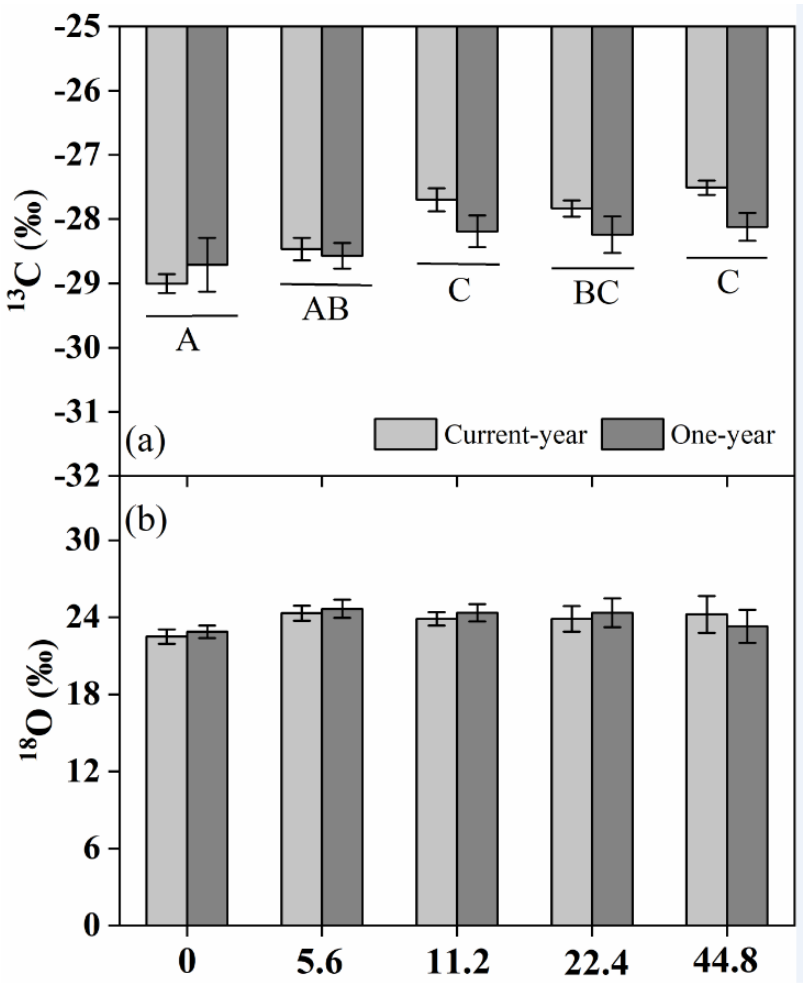

Fig. 4 Variations of $\delta^{13}C$ (a) and $\delta^{18}O$ (b) of current- and one-year old needles with different N addition rates (g N m^{-2} yr^{-1}). Values are means ± SE (n = 6). Different capital letters indicated significant differences among N treatments based on the results of mixed effect model shown in Table S2.

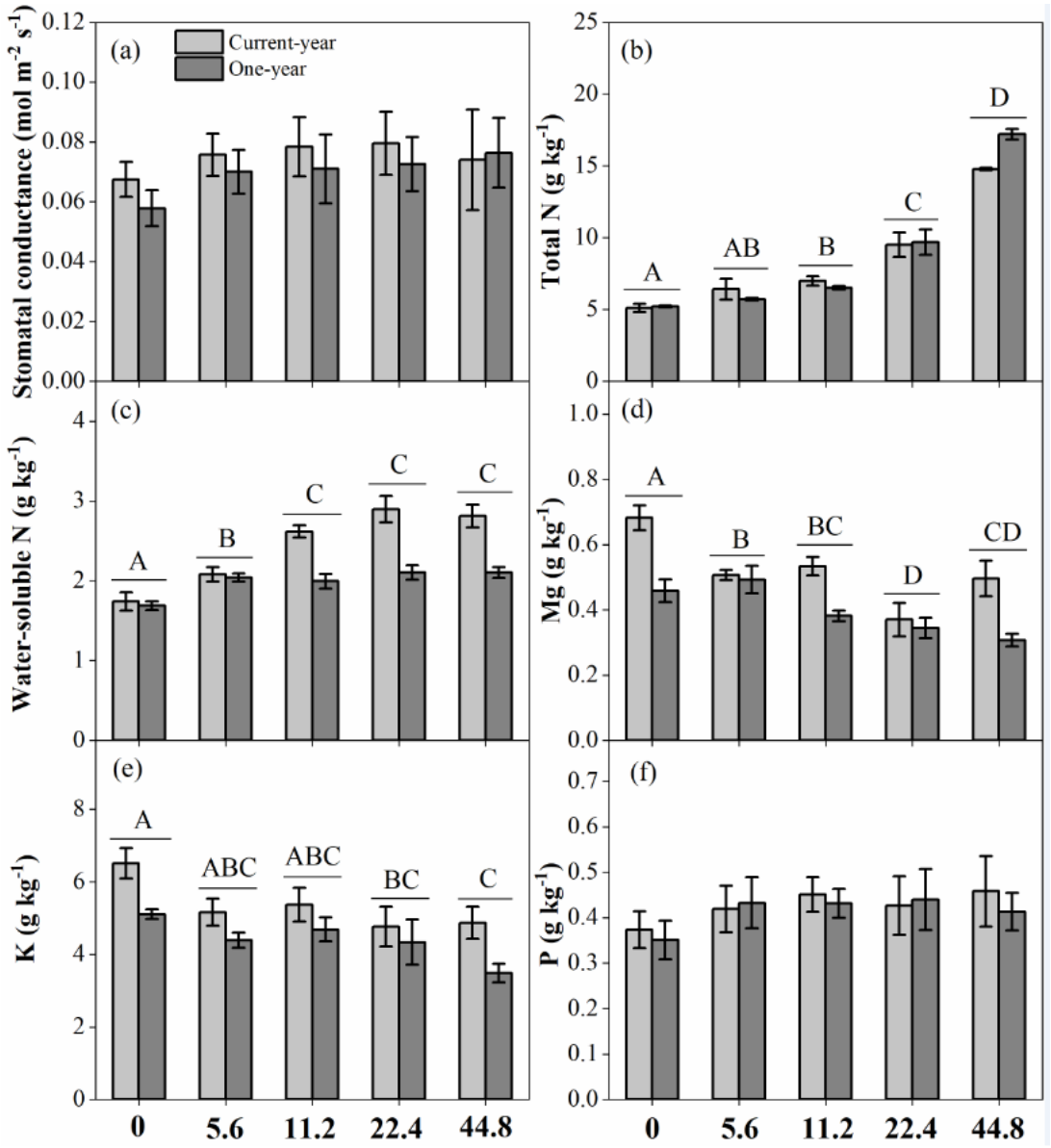

Fig. 5 Variations of stomatal conductance (a), total nitrogen (b), water-soluble nitrogen (c), magnesium (d), potassium (e), phosphorus (f) of current- and one-year old needles with different N addition rates (g N m^{-2} yr^{-1}). Values are means ± SE (n = 6). Different capital letters indicated significant differences among N treatments based on the results of mixed effect model shown in Table S3

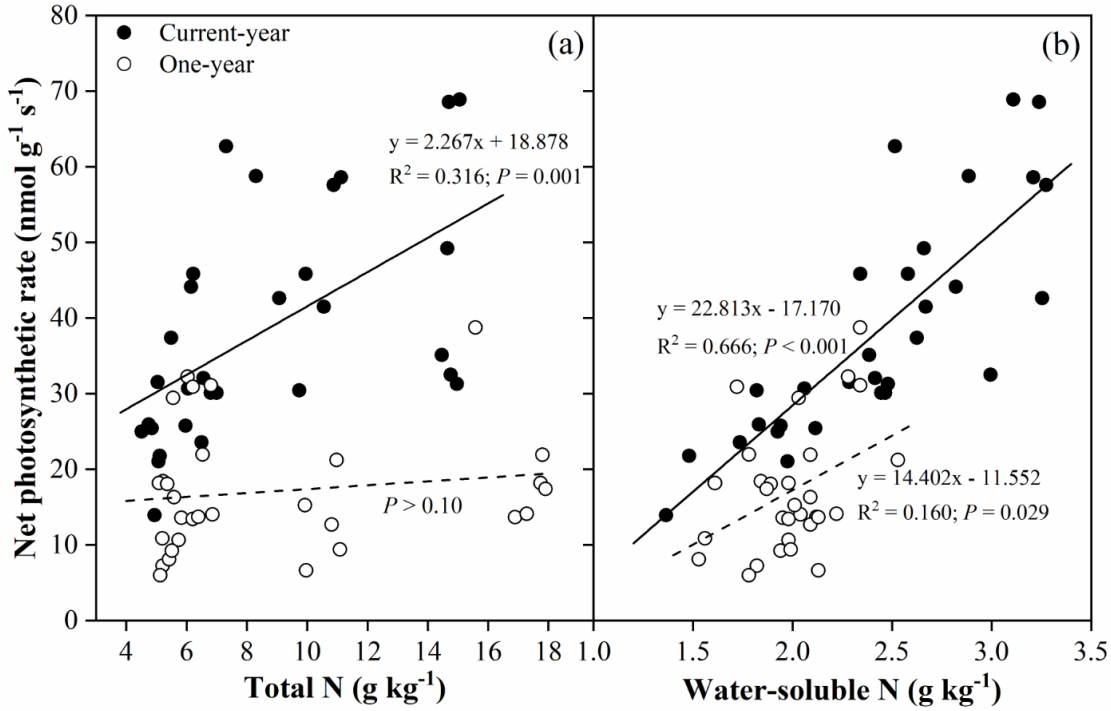

Fig. 6 Relationships between net photosynthetic rates and total N (a), and water-soluble N in needles (b). Solid lines are for current-year needles, and dashed lines are for one-year old needles.

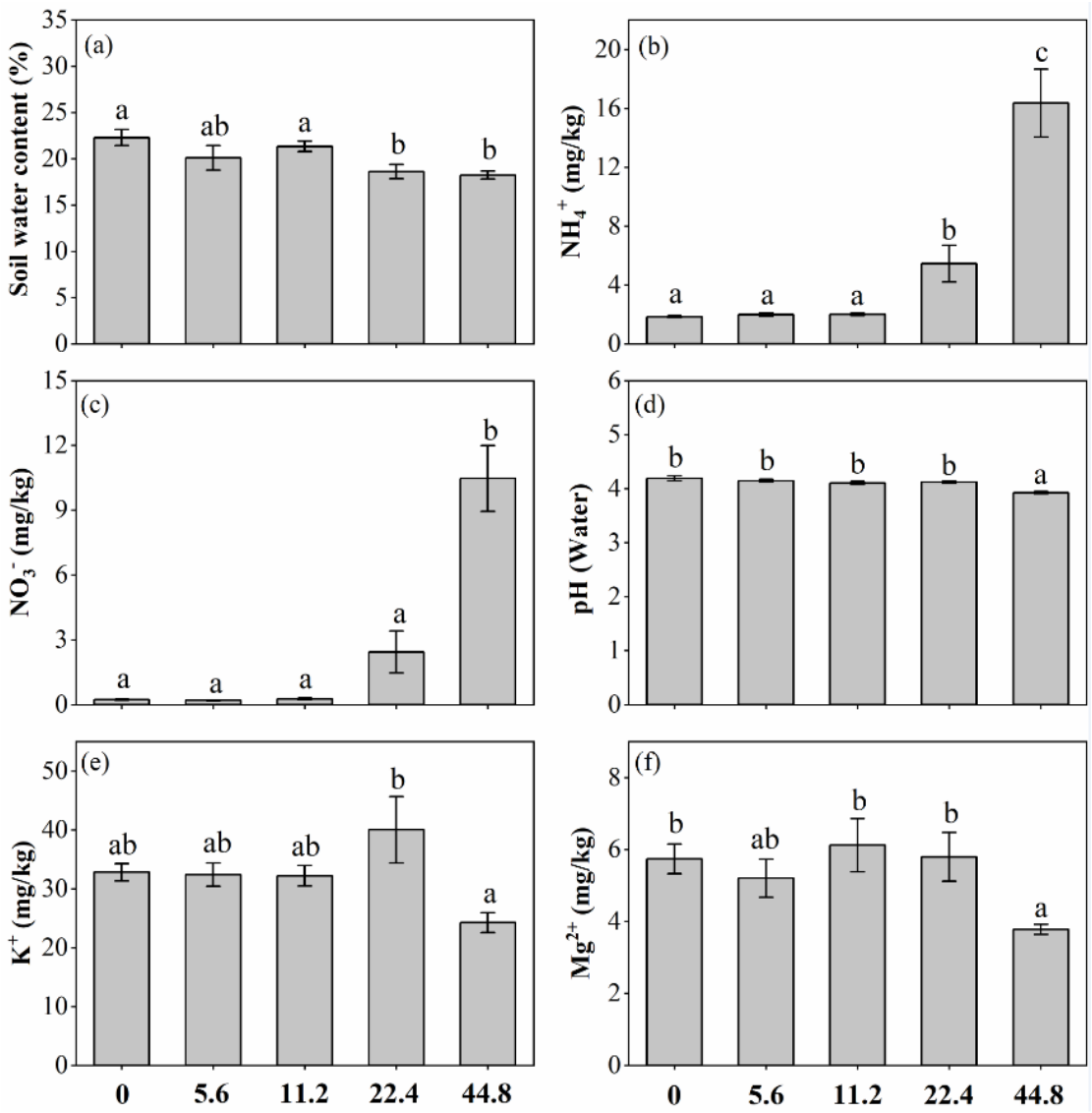

Fig. 7 Variations of water content (a), ammonium (b), nitrate (c), pH values (d), potassium ion (e), and magnesium ion (f) of soils received different rates of N addition (g N m^{-2} yr^{-1}). Values are means ± SE (n = 6). Different lowercase letters indicated significant differences among N treatments.

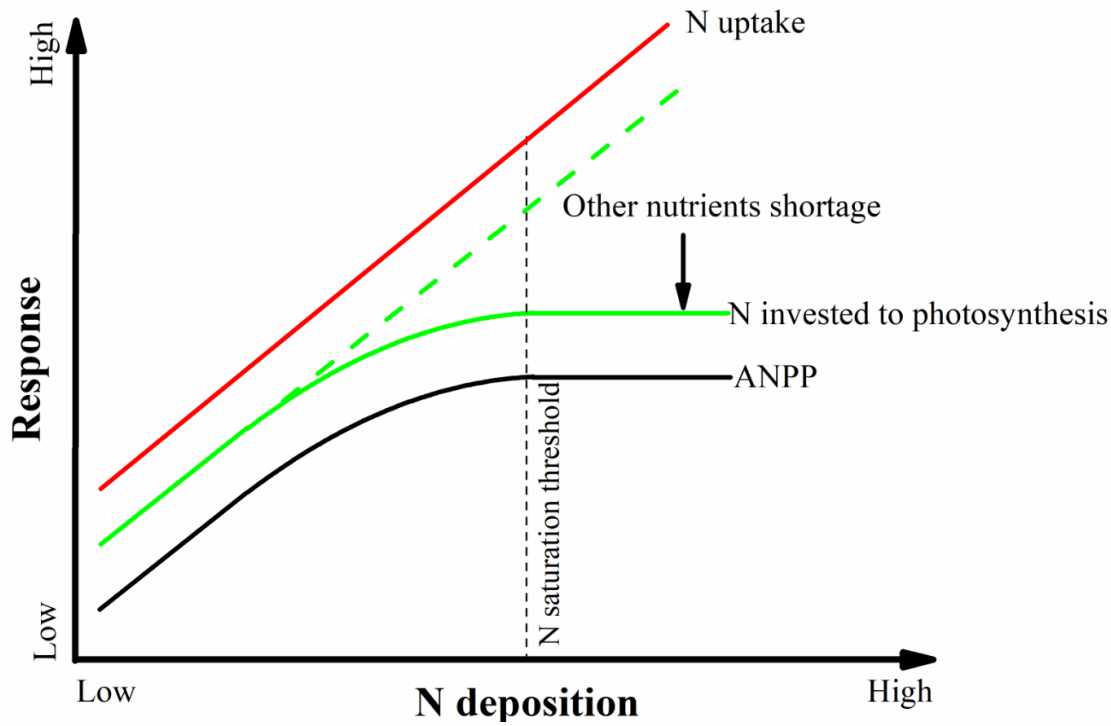

Fig. 8 The conceptual framework on the response of ANPP to continuously N input and the associated mechanisms. The red solid line indicates the continuously increased N uptake by trees with N deposition rates. The solid green and black lines having parallel trends indicate the nonlinear responses of needle N partitioning to photosynthesis and ANPP, respectively, to N addition. The gap between the dotted and solid green lines indicates the N gain by the trees that will not been invested to photosynthesis due to the shortage of nutrients other than N. The dotted black line indicates the N saturation threshold.

Table 1 Diameter at breast height (DBH) and height (H) of the trees under various N addition rates.

N addition rates ($g\ N\ m^{-2}\ yr^{-1}$)	July 2019		July 2020	
	DBH (cm)	H (m)	DBH (cm)	H (m)
0	2.32±0.02	2.33±0.04	3.15±0.04	2.94±0.03
5.6	2.73±0.15	2.55±0.11	3.79±0.16	3.26±0.08
11.2	2.58±0.17	2.46±0.09	3.90±0.13	3.12±0.15
22.4	2.55±0.17	2.41±0.07	3.90±0.19	3.05±0.07
44.8	2.93±0.08	2.51±0.03	4.38±0.09	3.10±0.02

Values are means ± standard errors (n = 6).

Table S1 Results of linear mixed effect model of N, needle age, and their interaction on needle light-saturated net photosynthetic rate.

Effect	*df*	Net photosynthetic rate	
		F	*P*
N	4, 25	6.26	**0.001**
Needle age	1, 25	44.83	**＜0.001**
N×Needle age	4, 25	2.57	**0.063**

Table S2 Results of linear mixed effect model of N, needle age, and their interaction on needle $\delta^{13}C$ and $\delta^{18}O$

Effect	*df*	$\delta^{13}C$		$\delta^{18}O$	
		F	*P*	*F*	*P*
N	4, 25	6.42	**0.001**	0.63	0.647
Needle age	1, 25	4.03	**0.056**	0.57	0.459
N×Needle age	4, 25	1.52	0.228	2.01	0.124

Table S3 Results of linear mixed effect model of N, needle age, and their interaction on needle stomatal conductance, total nitrogen, water-soluble nitrogen, magnesium, potassium, phosphorus

Effect	*df*	Stomatal conductance		Total N		Water-soluble N		Mg		K		P	
		F	*P*	*F*	*P*	*F*	*P*	*F*	*P*	*F*	*P*	*F*	*P*
N	4, 25	0.60	0.664	101.40	**＜0.001**	23.33	**＜0.001**	13.85	**＜0.001**	2.75	**0.050**	0.46	0.762
Needle age	1, 25	0.73	0.402	2.55	0.123	43.06	**＜0.001**	23.86	**＜0.001**	38.08	**＜0.001**	0.34	0.567
N×Needle age	4, 25	0.101	0.981	8.132	**＜0.001**	5.89	**0.002**	3.01	**0.037**	1.70	0.182	0.29	0.879